A Study of Evaporation Heat Transfer Coefficient Correlations at Low Heat and Mass Fluxes for Pure Refrigerants and Refrigerant Mixtures

M. K. Smith, J. P. Wattelet, and T. A. Newell

ACRC TR-32 January 1993

For additional information:

Air Conditioning and Refrigeration Center
University of Illinois
Mechanical & Industrial Engineering Dept.
1206 West Green Street
Urbana, IL 61801

(217) 333-3115

Prepared as part of ACRC Project 01
Refrigerant-Side Evaporation and Condensation Studies
J. C. Chato, Principal Investigator

The Air Conditioning and Refrigeration Center was founded in 1988 with a grant from the estate of Richard W. Kritzer, the founder of Peerless of America Inc. A State of Illinois Technology Challenge Grant helped build the laboratory facilities. The ACRC receives continuing support from the Richard W. Kritzer Endowment and the National Science Foundation. The following organizations have also become sponsors of the Center.

Acustar Division of Chrysler
Allied-Signal, Inc.
Amana Refrigeration, Inc.
Bergstrom Manufacturing Co.
Caterpillar, Inc.
E. I. du Pont de Nemours & Co.
Electric Power Research Institute
Ford Motor Company
General Electric Company
Harrison Division of GM
ICI Americas, Inc.
Johnson Controls, Inc.
Modine Manufacturing Co.
Peerless of America, Inc.
Environmental Protection Agency
U. S. Army CERL
Whirlpool Corporation

For additional information:

Air Conditioning & Refrigeration Center
Mechanical & Industrial Engineering Dept.
University of Illinois
1206 West Green Street
Urbana IL 61801

217 333 3115

A Study of Evaporation Heat Transfer Coefficient Correlations at Low Heat and Mass Fluxes for Pure Refrigerants and Refrigerant Mixtures

M. K. Smith, J. Wattelet and T. A. Newell
Dept. of Mech. Eng., University of Illinois, 1206 W. Green St., Urbana, IL 61821

Abstract

An average R12 refrigerant correlation has been developed for the mass flux range of 25-100 kg/m^2-s and the heat flux range of 2-10 kW/m^2. Refrigerant mixtures of 80% R22/20% R141b and 65% R22/35% R123 have also been tested over a similar range of conditions. Mixture heat transfer coefficients have been determined and correlations for each mixture pair are presented. The R22/R141b average correlation may have a strong dependence on changes in surface tension. The heat transfer coefficient of R22/R141b compares well with that of R12. The heat transfer coefficient of R22/R123 severely under performs R12.

Nomenclature

Bo - Boiling number

$$Bo = \frac{q}{Gi_{lg}}$$

Bond - Bond number

$$Bond = \frac{g(\rho_l - \rho_v)D^2}{\sigma} \approx \frac{We_l}{Fr_l}$$

Fr - Froude number of liquid

$$Fr_l = \frac{G^2}{\rho_l^2 gD}$$

K - Pierre boiling number

$$K = \frac{\Delta x \cdot i_{lg}}{len \cdot g}$$

Pr_l - Prandtl number of liquid

$$Pr_l = \frac{c_{p_l}\mu_l}{k_l}$$

Re_l - Reynolds number of liquid

$$Re_l = \frac{GD(1-x)}{\mu_l}$$

Re_{lo} - Reynolds number of liquid only

$$Re_{lo} = \frac{GD}{\mu_l}$$

We_l - Weber number of liquid

$$We_l = \frac{G^2 D}{\sigma \rho_l}$$

Symbols

C - Celsius
c_{pl} - specific heat of liquid (J/kg-K)
D - tube inside diameter (m)
g - acceleration of gravity (m/s^2)
G - mass flux (kg/m^2-s)
h - heat transfer coefficient (W/m^2-K)
$\bar{h}$ - average heat transfer coefficient (not quality dependent) (W/m^2-K)
h_l - heat transfer coefficient of the liquid from Dittus-Boelter correlation (W/m^2-K) [1]

$$h_l = 0.023\frac{k_l}{D}Re_l^{0.8}Pr_l^{0.4}$$

h_{lo} - heat transfer coefficient of the liquid only from Dittus-Boelter correlation (W/m^2-K) [1]

$$h_{lo} = 0.023\frac{k_l}{D}Re_{lo}^{0.8}Pr_l^{0.4}$$

i_{lg} - latent heat of vaporization (kJ/kg)
k_l - thermal conductivity of liquid (W/m-K)
len - length of heat exchanger (m)
q - heat flux (kW/m^2)
UIUC - University of Illinois at Urbana-Champaign
x - quality

Greek Symbols

Δx - change in quality across heat exchanger
μ_l - viscosity of liquid (kg/m-s)
ρ_l - density of liquid (kg/m^3)
ρ_v - density of vapor (kg/m^3)
σ - surface tension of liquid (N/m)

Introduction

Many refrigerant correlations are developed from data taken at mass and heat fluxes greater than 100 kg/m^{2}s and 10 kW/m^2, respectively. The dominate flow regime, at these conditions, is annular with nucleate boiling generally present at low qualities. These flow conditions typify those found in window air conditioners and heat pumps. Examining conditions relevant to domestic refrigerator-freezer evaporators where mass fluxes are below 60 kg/m^{2}s and heat fluxes are less than 2.5 kW/m^2 is the primary goal of this study. In this range, the flow is predominately wavy/stratified. A second goal of this paper is a discussion of non-azeotropic refrigerant mixture evaporation heat transfer coefficients. Two mixtures have been studied under conditions found in domestic refrigerator-freezer evaporators.

A new average R12 correlation, based on data from the University of Illinois at Urbana-Champaign (UIUC R12) evaporation test facility, has been developed for low heat flux and mass flux conditions. The heat transfer coefficients were obtained from a horizontal, single-tube evaporation test setup. The correlation is a function of the heat transfer coefficient of the liquid only, h_{lo}, and the boiling number, Bo. h_{lo} is calculated from the familiar Dittus-Boelter correlation [1]. The correlation gives an average versus a local value of the heat transfer coefficient; therefore, the quality does not appear in the correlation.

A discussion of this new correlation and existing correlations over a range of heat and mass fluxes is presented. The correlations of Jung and Radermacher [2], Kandlikar [3], Pierre [4] and Shah [5] were considered for comparison with the UIUC R12 correlation. Pierre's correlation and Shah's correlation are compared directly because they overlap with the range of interest.

The second part of the work presents results obtained from non-azeotropic refrigerant evaporation experiments. A domestic refrigerator-freezer evaporator test facility has been used for this work. The UIUC R12 correlation is used to obtain air-side heat transfer coefficients as a function of air velocity for two sizes of refrigerator evaporators in the test facility . The test facility consisted of a refrigerant loop loaded with R12 and two well-insulated evaporator compartments. Controlled conditions were maintained in each compartment and careful measurements of temperatures and mass flow rates permitted an energy balance to be performed on each compartment. Knowledge of the overall energy balance and the refrigerant heat transfer coefficient, from the UIUC R12 correlation, allowed direct calculation of an average air-side heat transfer coefficient. Tests were run over a systematic range of air flow rates.

Once evaporator air-side performance was characterized, the test loop was loaded with the refrigerant mixtures 65% R22/35% R123 and 80% R22/20% R141b. Knowledge of the overall energy balance and the air-side heat transfer coefficient from the evaporator tests allowed direct calculation of refrigerant heat transfer coefficients for a wide range of operating conditions. The heat transfer coefficient values obtained were fit to an appropriate correlation form. Several possible fits were explored. The final correlation forms for each mixture combination, 65% R22/R123 and 80% R22/R141b, are presented. A comparison of the mixture correlations and the UIUC R12 correlation was

performed. The less volatile mixture, R22/R123, did not perform as well as the more volatile mixture, R22/R141b.

UIUC R12 Correlation Development

A single-tube evaporator test facility has been developed at UIUC to measure evaporation characteristics of ozone-safe refrigerants. Testing has been conducted for low flow rates and heat fluxes similar to those found in household refrigerator evaporators. Results of high flow rates and heat flux tests, 100-500 kg/m^2-s and 5-30 kW/m^2, can be found in previous work by Wattelet *et al.* [6].

The test section consisted of a 7.04 mm, 2.43 m long copper tube. Heat was applied to the test section using electric resistance heaters. Test parameters were as follows: mass flux, 25-100 kg/m^{2}s; heat flux, 2-10 kW/m^2; quality, 20-90 percent; saturation temperature, -20 to 5 °C. Refrigerants R134a and R12 were used as the test fluids. Flow patterns were determined by strobe-light enhanced visual observation from sight glasses at the inlet and outlet of the test section. The predominate flow pattern was wavy-stratified flow.

Figure 1 is a plot of R12's heat transfer coefficient versus quality. There is no major effect of quality on the circumferentially averaged heat transfer coefficients. However, as the heat flux increases, the heat transfer coefficient also increases. Convective boiling is diminished while nucleate boiling does not appear to be suppressed at higher qualities or for lower heat fluxes.

For wavy-stratified flows, part of the wall perimeter remains dry, decreasing the area available for convective boiling at the liquid-vapor interface. Nucleate boiling can occur at the wetted wall perimeter. As shown in Figure 1, the effect of convective boiling does not vary with quality for a fixed mass flux and heat flux; therefore quality terms do not appear in the correlation for wavy-stratified flows. The transition from predominately wavy to predominately annular flow was found to be most influenced by mass flux. A Froude number, Fr_l, is suggested as the transition criteria. For $Fr_l < 0.10$, the wavy-stratified correlation should be used.

Equation 1 shows the form of the average heat transfer coefficient equation for R12 or R134a. The results for both fluids were identical.

$$\frac{\bar{h}}{h_{lo}} = 4.3 + 0.4\left(Bo \times 10^4\right)^{1.3} \qquad (1)$$

Comparison of UIUC R12 Correlation Against Other Correlations

A comparison of the UIUC R12 correlation was made to existing correlations found in the literature. The correlations of Jung and Radermacher [2], Kandlikar [3], Pierre [4] and Shah [5] were examined. Table 1 lists the applicable heat and mass flux ranges for these correlations. Figure 2 shows a map of heat flux vs. mass flux with the ranges of each correlation represented as shaded boxes. Four additional boxes are shown. Two of them show the heat and mass flux ranges for typical operation of refrigerators and room air-conditioners. The other two boxes show the ranges for the UIUC mixture

correlations and will be discussed in a later section. Jung's range is typical of heat pumps.

Of the four correlations, Jung, Kandlikar, Pierre and Shah, only Pierre's and Shah's correlations overlap the UIUC R12 correlation. Both correlations were developed with tubes 50 percent or larger in diameter than is typically used for domestic refrigerator-evaporators. Pierre's correlation, Equation 2, is an average correlation developed specifically for R12 and covers the entire range of the UIUC correlation.

$$\bar{h} = 0.00097 \frac{k_l}{D} Re_{lo} K^{0.5} \qquad (2)$$

K is a boiling number defined by Pierre.

Shah's correlation is a generalized local correlation. For this correlation, data was gathered from nineteen independent experimental studies which covered eight different fluids. In addition, Jung's and Kandlikar's correlations are general correlations. To be accurately compared to the UIUC R12 average correlation, Shah's correlation was numerically integrated, as shown in Equation 3, over the quality range of 0.1 to 0.9 to obtain an average heat transfer coefficient.

$$\bar{h} = \frac{1}{x - x_o} \int_{x_o}^{x} h dx \qquad (3)$$

Shah's correlation will not be presented here. If interested, please check reference [5].

Looking again at Figure 2, the ranges of Pierre's and Shah's correlations are large, encompassing at least a part of the operating ranges of refrigerators, room air conditioners and heat pumps. It would be expected that these correlations would not be as accurate as a correlation specifically targeted for one of these ranges. There is a flow regime transition from the low mass flux refrigerator operating range to the high mass flux heat pump operating range of stratified/wavy to annular flow. Even within a specific range there can be large differences in Bo number and thus the possible onset of nucleate boiling at the wetted tube wall. On the chart, Bo number increases up and to the left and decreases down and to the right.

Figure 3 is a graph showing a comparison of the UIUC R12, Pierre's R12 correlation, and Shah's correlation with UIUC experimental heat transfer coefficients. The mass flux and heat flux range over which the comparison was performed was that of the UIUC R12 correlation, G = 25 - 100 kg/m^2-s and q = 2 - 10 kW/m^2. The saturation temperature was -10 degrees C. The three lines on the graph are the +20%, 0% and -20% error bounds.

All three correlations predict R12 heat transfer coeeficients with reasonable accuracy over the entire range of realtively low heat flux/mass flow conditions. Shah's correlation shows somewhat broader scatter with deviations greater than 20 percent at the lower heat transfer coefficient range, however, given the relatively broad range of data used to derived the correlation, it is generally within acceptable accuracy. The tendency of Pierre's and Shah's correlations to underpredict transfer coefficients at the low end may be due to lack of nucleate boiling effects in their correlations.

Use of UIUC R12 Correlation to Determine Air-side Characteristics of Evaporators

A heat exchanger such as an evaporator can be characterized by its UA value. Knowing the inlet/outlet air and refrigerant temperatures and the evaporator load, the UA value can be calculated from:

$$UA = \frac{Q}{LMTD} \quad \text{where} \quad LMTD = \frac{\Delta T_1 - \Delta T_2}{\ln(\Delta T_2/\Delta T_1)} \tag{4}$$

Neglecting the small tube resistance, an alternate expression for UA can be written:

$$\frac{1}{UA} = \frac{1}{h_{air}A_{air}} + \frac{1}{h_{ref}A_{ref}} \tag{5}$$

With the knowledge of the evaporator geometry, the UA value and h_{ref}, an average air-side heat transfer coefficient can be calculated.

Two evaporators, an eight pass and a four pass evaporator, were constructed at the U of I (University of Illinois) and simultaneously tested. The eight pass evaporator transferred heat in the quality range of approximately 0.0 to 0.5 and the four pass evaporator transferred heat in the quality range of approximately 0.5 to 1.0. With separate heat exchangers, the effect of quality change and heat flux could be independently studied.

The tests were carried out in an evaporator test facility with its own independent refrigeration loop. The evaporators were placed in well insulated compartments of known thermal properties. R12 was loaded into the refrigeration loop and a series of tests were performed for various air velocities and refrigerant conditions. (The well insulated compartments were actually a refrigerator mock up built out of foam board. The walls are four inches thick with an approximate R value of 28. The dimensions of the compartments are similar to those of an 18 cubic foot refrigerator.)

Using the UIUC R12 correlation, the air side heat transfer coefficients were calculated from Equation 5. Figure 4 shows a plot of the air-side heat transfer coefficient of the four and eight pass evaporator over a wide range of air velocities. The four pass evaporator has greater air-side heat transfer coefficients over the tested velocity range than the eight pass evaporator. The difference is due to partial blockage of the air flow over subsequent tubes by the first few tubes.

Calculation of Mixture Heat Transfer Coefficient and Correlation Development

Two sets of mixture tests were performed. The first set was with the mixture 80% R22/20% R141b and the second set was with the mixture 65% R22/35% R123. Figure 2 shows the mass and heat flux ranges over which both of the sets of tests were performed. The R22/R141b tests were over a larger range of heat fluxes, whereas the R22/R123 tests were over a larger range of mass fluxes.

The loop was run at a variety of refrigerant conditions and air velocities. With knowledge of the air-side heat transfer coefficient and the physical dimensions of the heat exchanger, the refrigerant heat

transfer coefficients were able to be calculated from Equation 5. After the runs were complete, an attempt to correlate the data was made. Figure 5 and 6 show the plots of the correlated heat transfer coefficient plotted against the measured heat transfer coefficient with +20%, 0% and -20% error lines. For Figure 5, the R22/R141b plot, the data points show a fair amount of scatter. Figure 6, the R22/R123 plot, shows trends in the data at low heat transfer coefficient values. The slope of the trends is horizontal indicating that variation of the heat transfer coefficient has been compromised by the exclusion of an important variable such as quality.

Several correlation forms were tried similar to the previous correlations referred to in this paper. The average correlations for R22/R141b and R22/R123 are shown in Equations 6 and 7, respectively.

$$\bar{h}/h_{lo} = \exp(-16.617)\mathbf{Bond}^{6.1}\mathbf{Bo}^{0.7} \qquad (6)$$

$$\bar{h}/h_{lo} = \exp(-3.723)\mathbf{Bond}^{1.4}\mathbf{Bo}^{0.1} \qquad (7)$$

The correlations contain two non-dimensional numbers. The Bo number is present to account for the change in the heat transfer coefficient with heat flux. The Bo number dependence for R22/R141b is much greater than for the R22/R123 mixture. The R22/R141b mixture is 80% R22, whereas the R22/R123 mixture is only 65% R22. R22 is the volatile component of both mixtures; therefore the greater dependency on Bo number is associated with more volatile mixture, R22/R141b. (Note: The R22/R141b mixture was also tested over a wider range of heat flux.)

The Bond number was found to be the best non-dimensional number to used on the basis of trial and error. These mixtures exhibit slightly higher values of surface tension compared to R12. R22/R123's surface tension is 1.5% greater and R22/R141b's surface tension is 7.7% greater than R12 at an evaporating temperature of -10 degrees C. Since the major component of the mixtures is R22, the mixtures have a larger capacity than R12. The runs were performed on a equal load basis; consequently, the mass fluxes for the mixtures were less than R12. Reduced mass flux and greater values of surface tension could lead to wave suppression on the refrigerant vapor/liquid interface. This wave suppression could have impact on the convective evaporation component of the heat transfer coefficient. The strong dependence of R22/R141b on Bond number is due to its higher surface tension.

Looking closely at Figures 5 and 6, the fit is not especially good. One could argue that the use of an average heat transfer coefficient correlation is not appropriate if the mixture is characterized by a large temperature glide. (The temperature glide is the amount the saturation temperature changes across the saturation dome.) Large differences in property values cannot be accounted for with an average correlation. A second attempt was made to fit the data with a correlation form that was quality dependent in an effort to capture the property change due to the temperature glide. Instead of h_{lo} appearing in the correlation, h_l appears to account for the quality dependence. The local correlations for R22/R141b and R22/R123 are shown in Equations 8 and 9, respectively.

$$\mathbf{h} = \exp(16.14)\mathbf{h}_l^{0.41}\mathbf{Fr}^{2.4}\mathbf{We}^{-1.9}\mathbf{Bo}^{0.28} \qquad (8)$$

$$\mathbf{h} = \exp(4.33)\mathbf{h}_l^{0.23}\mathbf{Fr}^{-1.9}\mathbf{We}^{2.6}\mathbf{Bo}^{0.76} \qquad (9)$$

The We and Fr number dependence come from the Bond number dependence in Equations 6 and 7. The ratio of the We number to the Fr number is essentially the Bond number. Greater correlation dependence is on the Bo number for the R22/R141b mixture.

Figures 7 and 8 are plots of the measured vs. correlated heat transfer coefficient values. Error lines of +20%, 0% and -20% are drawn on the plots. For the R22/R141b mixture, Figure 7, not much improvement can be seen between the average and local correlation. The scatter pattern remains unchanged implying that the change in transfer coefficient value is essentially independent of quality. The R22/R123 plot, Figure 8, shows significant improvement in the area which had the horizontal trends discussed earlier in this section. When quality was introduced back into the correlation, data that was previously horizontal, lines up with the 0% error line. This indicates that the R22/R123 mixture is dependent on quality and that a local correlation is best.

Comparison of Mixture Correlations to the UIUC R12 Correlation

Figure 9 shows a comparison of the average mixture correlations with the UIUC R12 correlation. The comparison was done over a heat and mass flux range that was common to all three fluids (check Figure 2). The R22/ 141b mixture performs well against R12. Unfortunately, R22/R123 significantly under performs R12.

As pointed out earlier, the R22/R123 mixture is only 65% R22. It is less volatile than the R22/R141b mixture, which is 80% R22. At these relatively low values of heat flux, nucleate boiling is further suppressed for the R22/R123. Mass diffusion effects lower the superheat at the wetted wall. The more volatile component R22 is driven away from the wall region leaving an enriched mixture of the higher boiling point R123 near the wall, thus lowering the effective amount of superheat.

Conclusions

Heat transfer effects for some pure refrigerants and refrigerant mixtures have been examined in a range of heat fluxes and mass flow rates that are representative of domestic refrigerator-freezers. Typical refrigerator mass fluxes are 60 kg/m^2-s or less and typical heat fluxes are 2.5 kW/m^2 or less. An average correlation for R12 and R134a has been presented for a mass flux range of 25-100 kg/m^2-s and a heat flux range of 2-10 kW/m^2. This correlation is valuable as a design tool for the domestic refrigeration industry.

Examination of two non-azeotropic mixtures shows that heat transfer characteristics may have significantly different characteristics. The less volatile mixture, R22/R123, has a quality dependence and its heat transfer coefficient severely under performs that of R12, whereas the more volatile mixture, R22/R141b, does not have a significant quality dependence and its heat transfer coefficient compares well with that of R12.

Note 1

Since the mixture properties used for the development of the correlation are calculated and not measured, there is uncertainty in these values. The availability of measured physical property for mixtures is very limited; therefore, the liquid physical properties were calculated from mixture rules and the gaseous physical properties were calculated from the theory of corresponding states for gases as presented by Jung and Radermacher. [7]

Note 2

The mixture data was gathered in a indirect manner. Typical correlations are created from data taken from a horizontal tube evaporation test stand, as was the case for the UIUC R12 correlation presented in the first section. The mixture data was gathered from a real multi-pass evaporator operating under real refrigerator conditions. Flow patterns in a real evaporator, as opposed to a horizontal tube, are quite different. Observations made of a glass evaporator at UIUC [8] have documented that flow transitions do occur at the return bends in the evaporator. For stratified flow, transitions to annular flow occur immediately after the return bends and persists for about 1/10th the tube length. These flow transitions will have an effect on the correlation form.

Acknowledgments

Bob Hendricks at the United States Environmental Protection Agency and the Air Conditioning and Refrigeration Center at the University of Illinois Department of Mechanical and Industrial Engineering.

References

1 Dittus, F. W., and L. M. K. Boelter, University of California Publications on Engineering, Vol. 2, p. 443, Berkeley, 1930.

2 Jung, D.S. and R. Radermacher, "Prediction of Heat Transfer Coefficients of Various Refrigerants During Evaporation", ASHRAE Transactions, V. 97, Pt. 2.

3 Kandlikar, S.G., "A General Correlation for Saturated Two-Phase Boiling Heat Transfer Inside Horizontal and Vertical Tubes", Journal of Heat Transfer, Vol. 112, February 1990, pp. 219-228.

4 Pierre, B., "The Coefficient of Heat Transfer for Boiling Freon-12 in Horizontal Tubes", Heating and Air Treatment Engineer, December, 1956, pp. 302-310.

5 Shah, M.M., "Chart Correlation for Saturated Boiling Heat Transfer: Equations and Further Study", ASHRAE Transactions, Vol. 88, Part 1, pp. 185-196.

6 Wattelet, J., J. M. Saiz Jabardo, J. C. Chato, J. S. Panek and A. L. Souza, "Experimental Evaluation of Convective Boiling of Refrigerants HFC-134a and CFC-12", 28th National Heat Transfer Conference of the ASME, Two-Phase Flow and Heat Transfer, 1992, Vol HTD-Vol 197, pp. 121-127.

7 Jung. D. and R. Radermacher, "Transport Properties and Surface Tension of Pure and Mixed Refrigerants", ASHRAE Transactions, V. 97, Pt. 1.

8 Barnhart, J., "A n Experimental Investigation of Flow Patterns and Liquid Entrainment in a

Horizontal Tube Evaporator", Ph.D. Thesis, Department of Mechanical Engineering, University of Illinois, December, 1992.

List of Figures

Figure 1. Heat transfer coefficient versus quality for wavy-stratified flow during flow boiling. Mass flux, 50 kg/m^{2}s; Saturation temperature, 5 °C; Tube diameter, 7.04 mm; Refrigerant R12.

Figure 2. Map of heat flux versus mass flux. Shows the range of applicability of various correlations and the operation ranges of refrigerators and room air-conditioners.

Figure 3. Shah and Pierre correlation heat transfer coefficients versus UIUC R12 correlation heat transfer coefficient. Mass flux, 25-100 kg/m^2-s by 15 kg/m^2-s increments; Heat flux 2-10 kW/m^2 by 1 kW/m^2 increments; Saturation temperature, -10 °C; Tube diameter, 7.9 mm.

Figure 4. Air heat transfer coefficients for an eight pass and a four pass evaporator versus air velocity.

Figure 5. 80% R22/20% R141b average correlated heat transfer coefficient versus measured heat transfer coefficient. Mass flux, 25-42 kg/m^2-s; Heat flux 1.0-4.2 kW/m^2; Tube diameter, 7.9 mm.

Figure 6. 65% R22/35% R123 average correlated heat transfer coefficient versus measured heat transfer coefficient. Mass flux, 25-85 kg/m^2-s; Heat flux 1.2-2.8 kW/m^2; Tube diameter, 7.9 mm.

Figure 7. 80% R22/20% R141b local correlated heat transfer coefficient versus measured heat transfer coefficient. Mass flux, 25-42 kg/m^2-s; Heat flux 1.0-4.2 kW/m^2; Tube diameter, 7.9 mm.

Figure 8. 65% R22/35% R123 local correlated heat transfer coefficient versus measured heat transfer coefficient. Mass flux, 25-85 kg/m^2-s; Heat flux 1.2-2.8 kW/m^2; Tube diameter, 7.9 mm.

Figure 9. 80% R22/20% R141b and 65% R22/35% R123 average correlation heat transfer coefficients versus UIUC R12 correlation heat transfer coefficient. Mass flux, 25-45 kg/m^2-s by 10 kg/m^2-s increments; Heat flux 2-2.8 kW/m^2 by 0.2 kW/m^2 increments; Effective saturation temperature, -10 °C; Tube diameter, 7.9 mm.

Table

TABLE 1

Correlation	G (kg/m^2-s)	q (kW/m^2)	Tube ID.(mm)
UIUC R12	25.0-100.0	2.0-10.0	7.04
Jung	250.0-720.0	10.0-45.0	9.1
Kandlikar	104.0-4479.0	0.3-80.0	6.66, 18.85, 20.0
Pierre	16.4-343.9	0.93-34.9	12.0, 18.0
Shah	13.6-582.9	1.58-34.7	11.68, 14.45, 14.66
UIUC R22/R141b	25.0-42.0	1.0-4.2	7.9
UIUC R22/R123	25.0-85.0	1.2-2.8	7.9

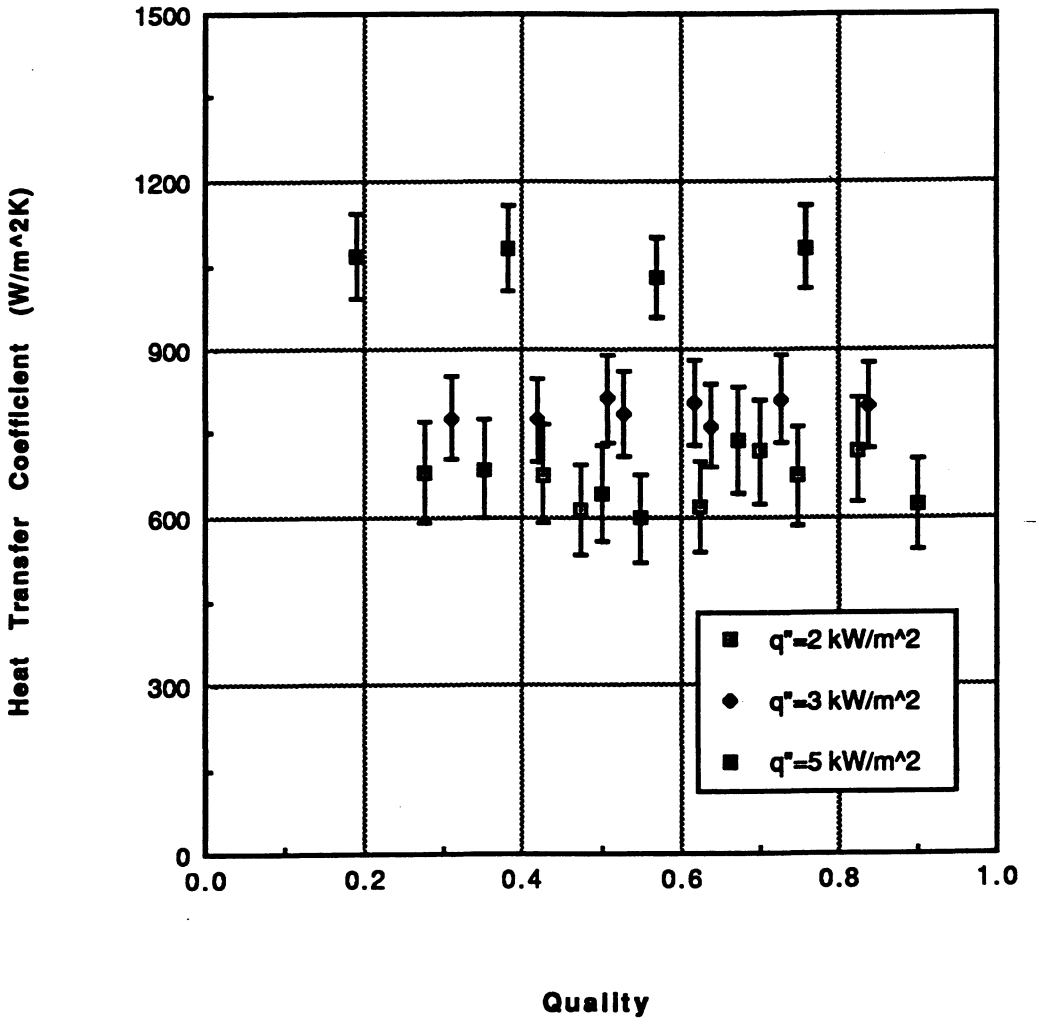
Heat Transfer Coefficient (W/m^2K)
1500
1200
900
600
300
0
0.0
0.2
0.4
0.6
0.8
1.0
Quality
q"=2 kW/m^2
q"=3 kW/m^2
q"=5 kW/m^2

FIG 1

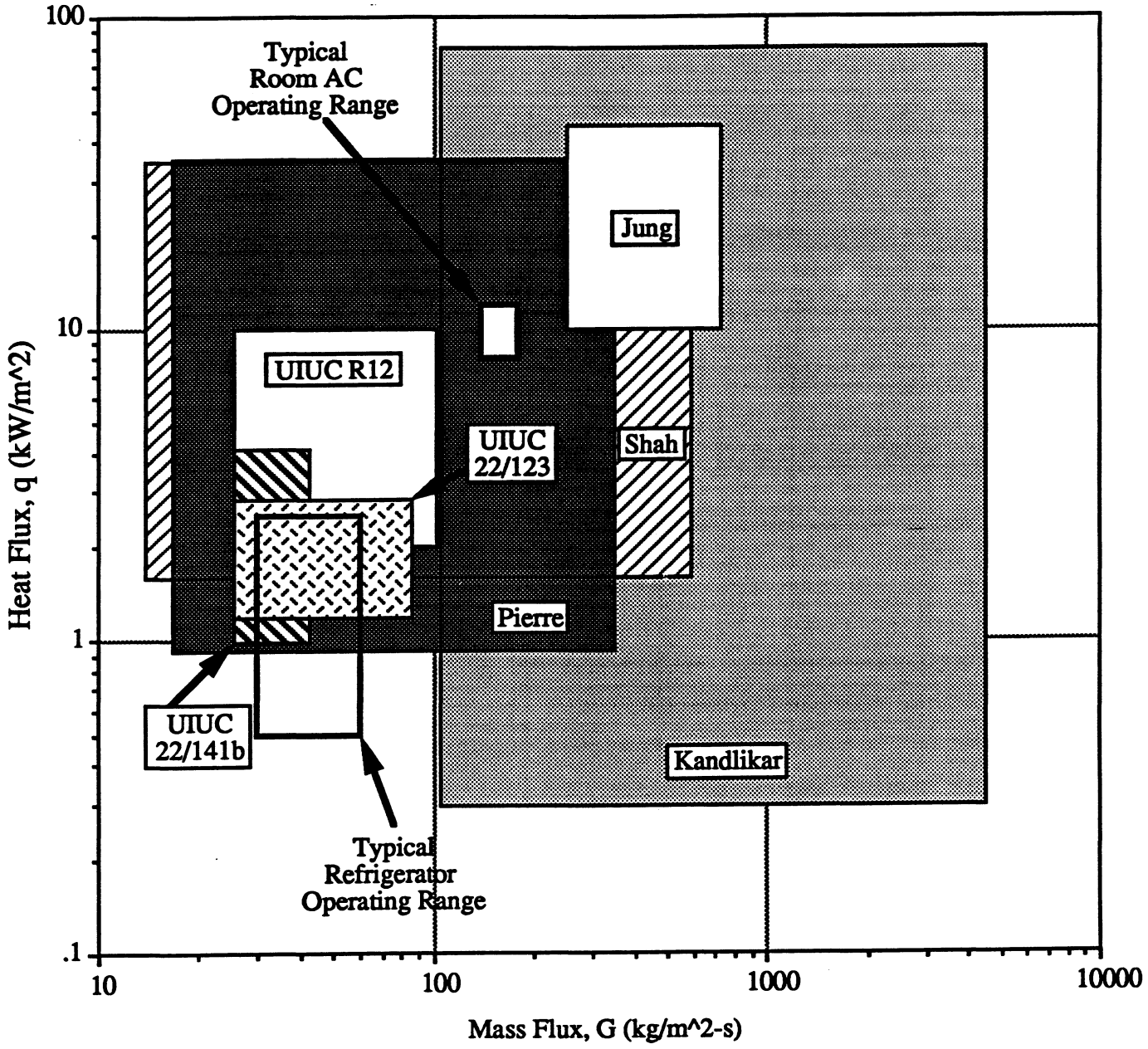
100
10
1
.1
Heat Flux, q (kW/m^2)
10
100
1000
10000
Mass Flux, G (kg/m^2-s)
Typical
Room AC
Operating Range
Jung
UIUC R12
UIUC
22/123
Shah
Pierre
UIUC
22/141b
Kandlikar
Typical
Refrigerator
Operating Range

FIG 2

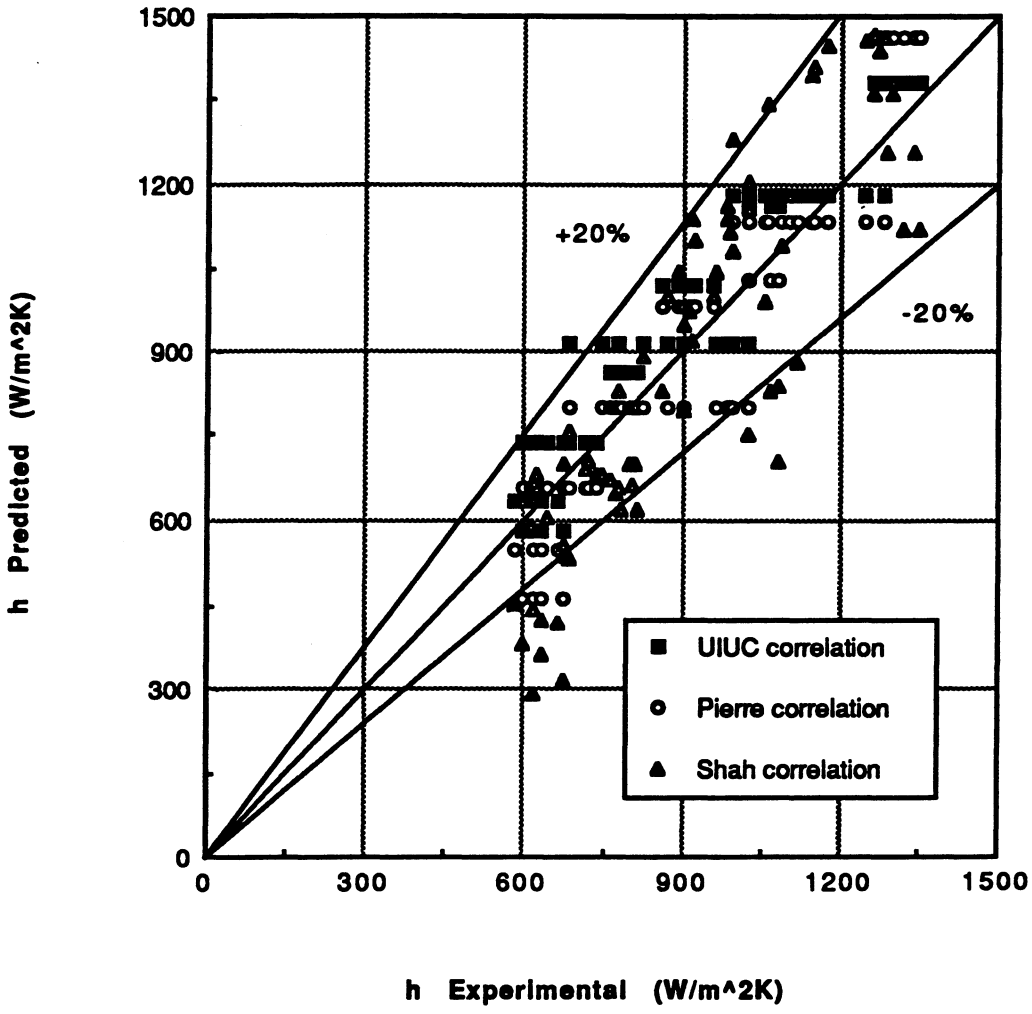
1500
1200
900
600
300
0
0
300
600
900
1200
1500
+20%
-20%
UIUC correlation
Pierre correlation
Shah correlation
h Predicted (W/m^2K)
h Experimental (W/m^2K)

FIG 3

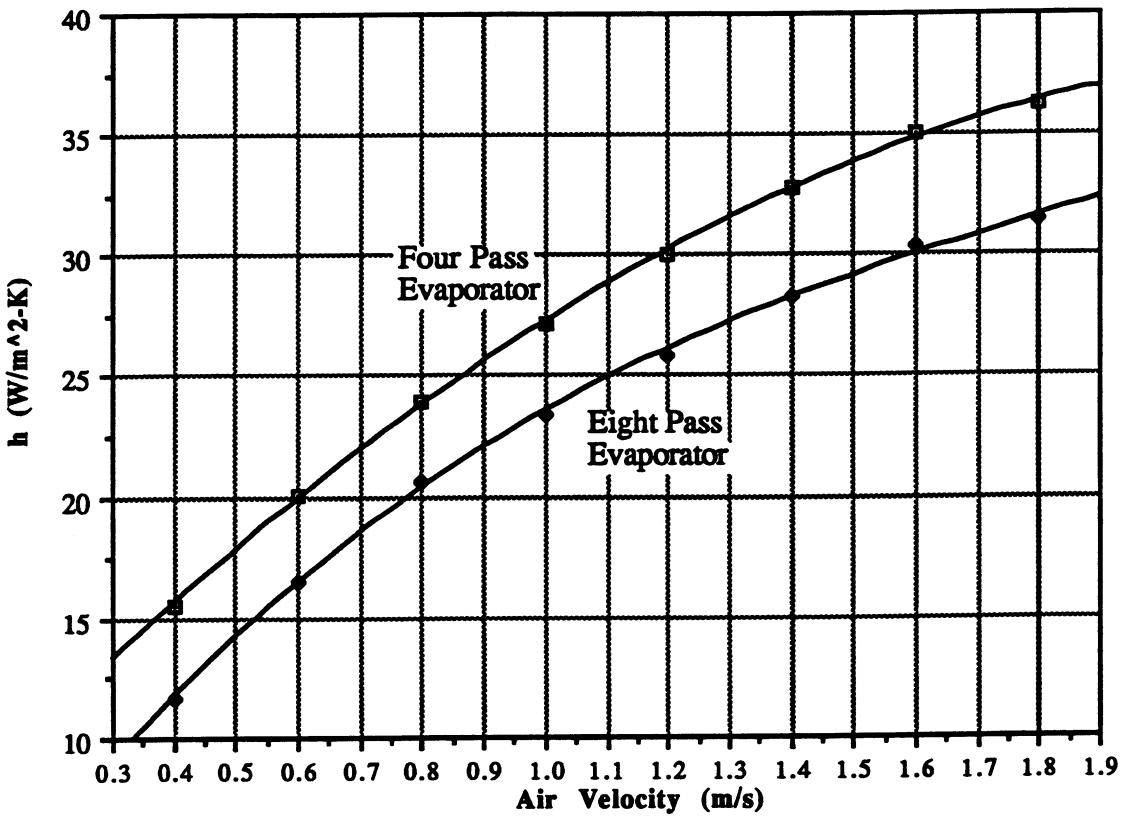
40
35
30
25
20
15
10
h (W/m^2-K)
Four Pass
Evaporator
Eight Pass
Evaporator
0.3 0.4 0.5 0.6 0.7 0.8 0.9 1.0 1.1 1.2 1.3 1.4 1.5 1.6 1.7 1.8 1.9
Air Velocity (m/s)

FIG 4

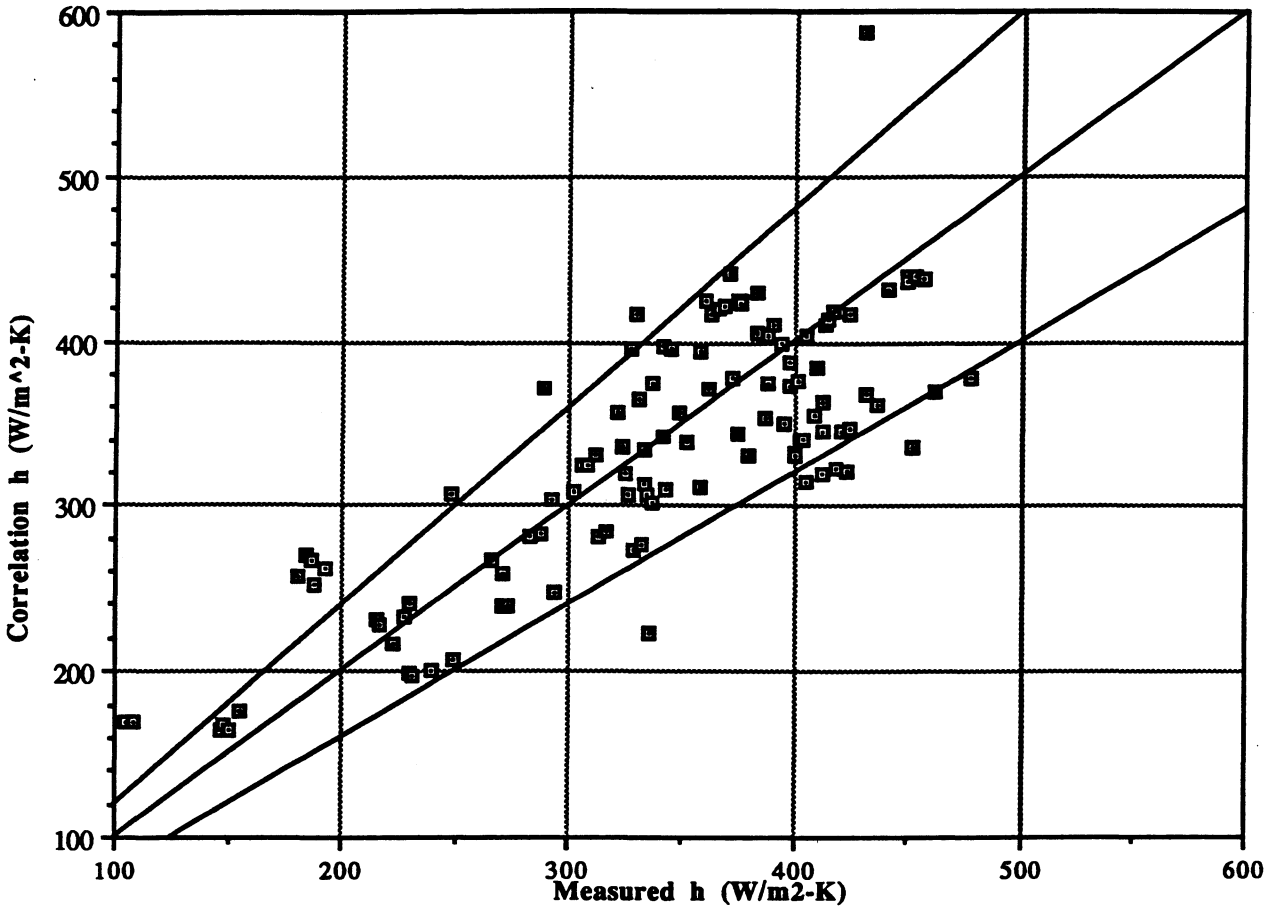
600
500
400
300
200
100
Correlation h (W/m^2-K)
100
200
300
400
500
600
Measured h (W/m2-K)

FIG 5

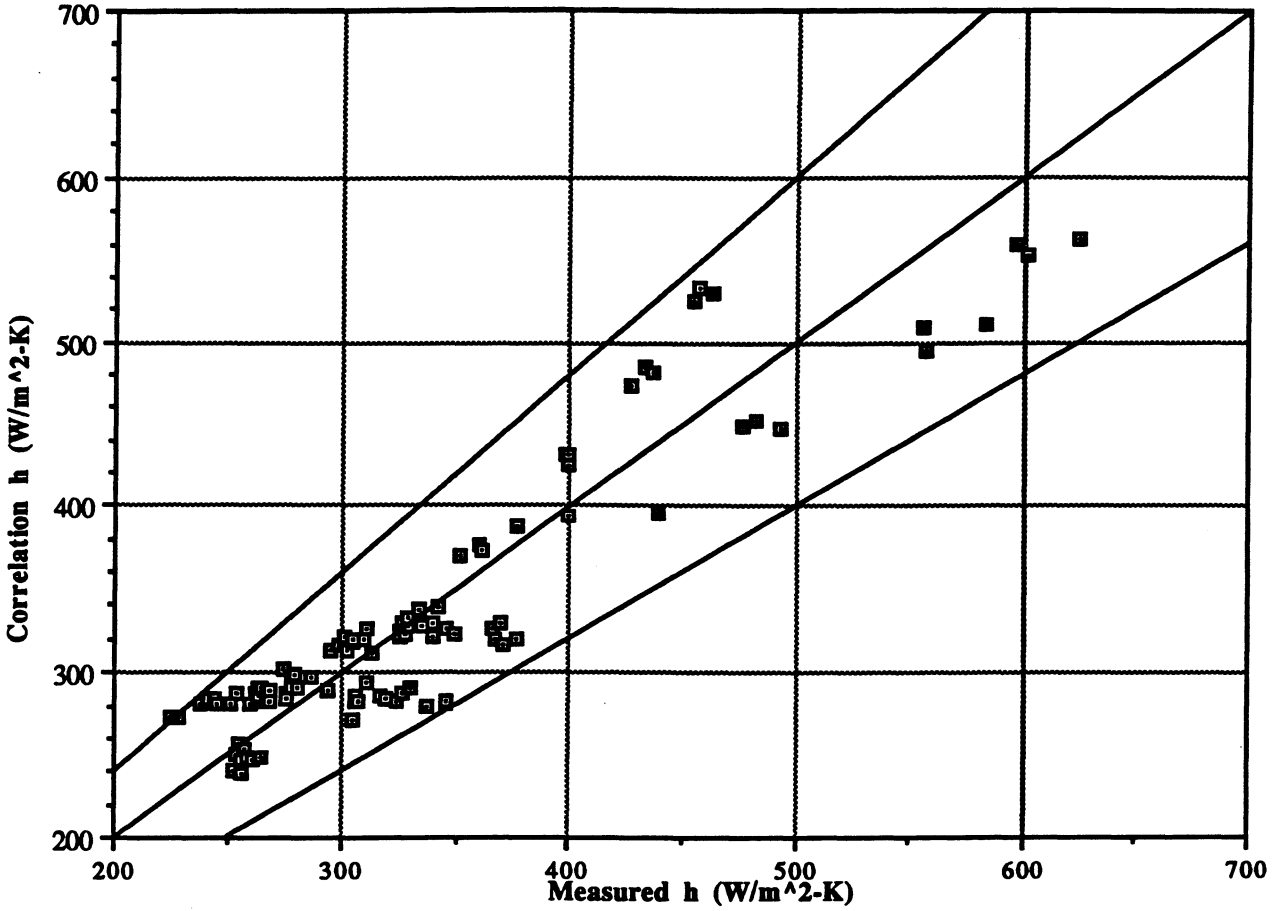
700
600
500
400
300
200
Correlation h (W/m^2-K)
200
300
400
500
600
700
Measured h (W/m^2-K)

FIG 6

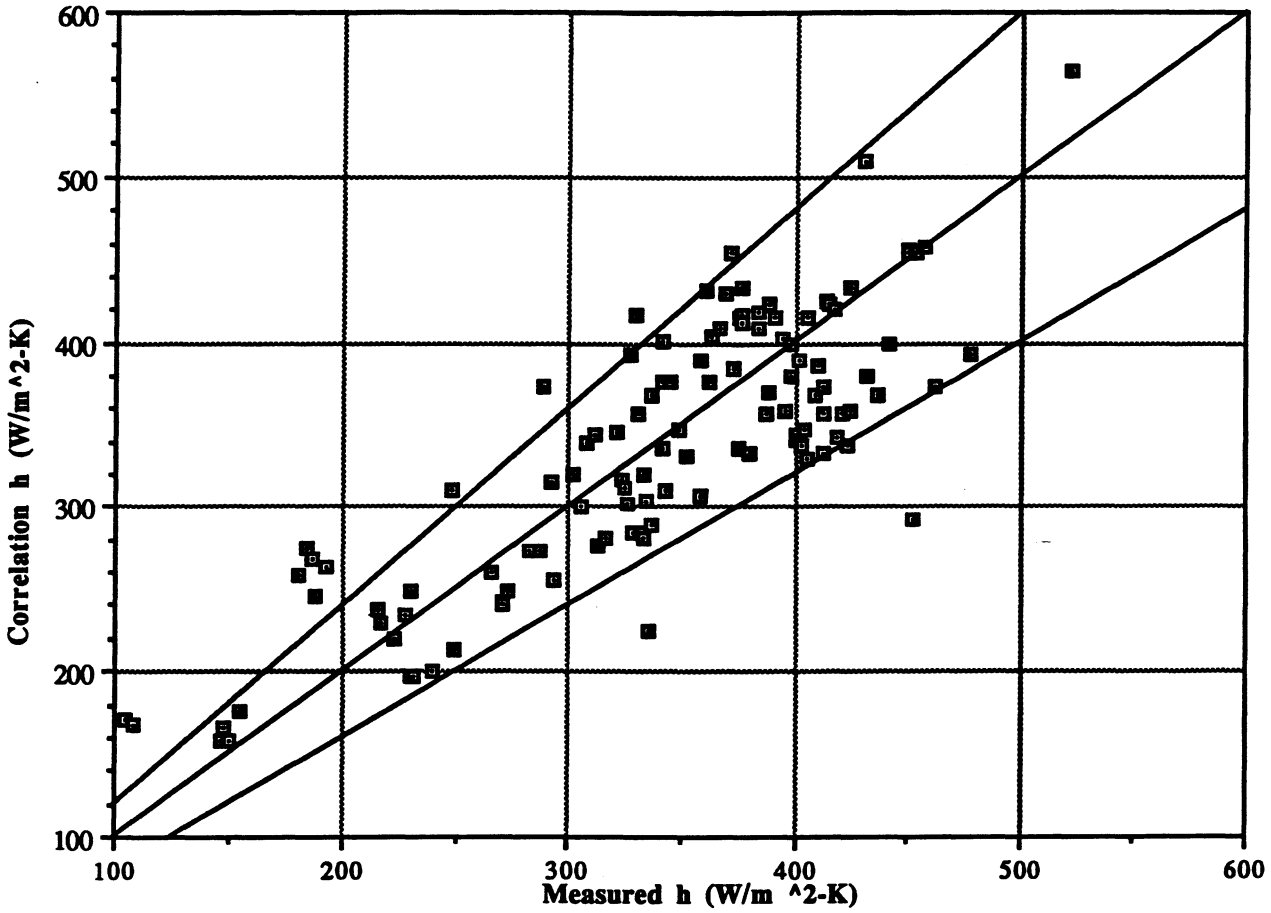
600
500
400
300
200
100
Correlation h (W/m^2-K)
100
200
300
400
500
600
Measured h (W/m ^2-K)

FIG 7

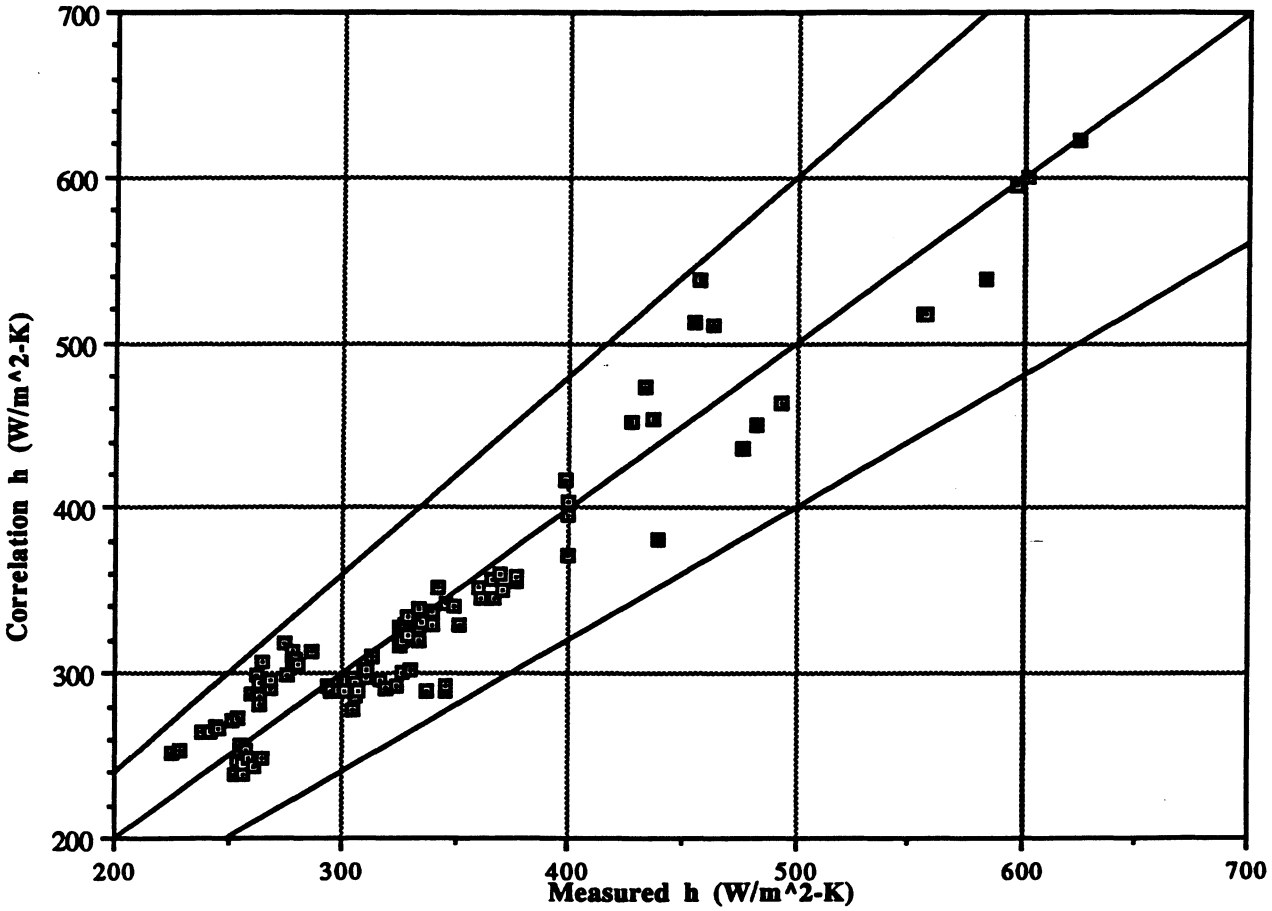
700
600
500
400
300
200
Correlation h (W/m^2-K)
200
300
400
500
600
700
Measured h (W/m^2-K)

FIG 8

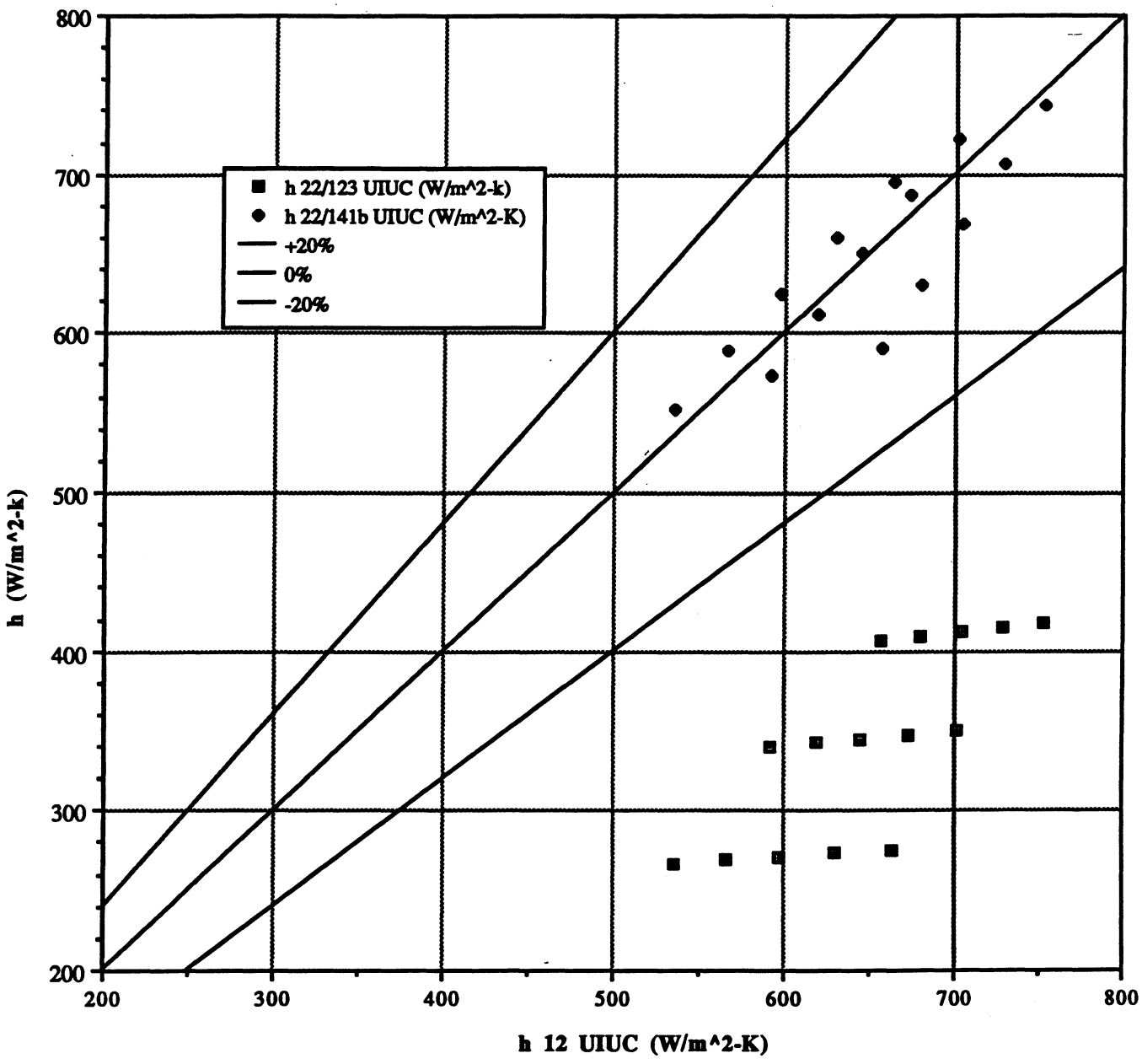
h 22/123 UIUC (W/m^2-k)
h 22/141b UIUC (W/m^2-K)
+20%
0%
-20%
h (W/m^2-k)
h 12 UIUC (W/m^2-K)
200
300
400
500
600
700
800

FIG 9